Chaos, Solitons and Fractals 91 (2016) 478–489

Contents lists available at ScienceDirect

Chaos, Solitons and Fractals

Nonlinear Science, and Nonequilibrium and Complex Phenomena

journal homepage: www.elsevier.com/locate/chaos

Frontiers

Old wine in fractal bottles I: Orthogonal expansions on self-referential spaces via fractal transformations

Christoph Bandt[a], Michael Barnsley[b,*], Markus Hegland[b], Andrew Vince[c]

[a] University of Greifswald, Germany
[b] Australian National University, Australia
[c] University of Florida and Australian National University, Australia

ARTICLE INFO

Article history:
Received 30 September 2015
Revised 11 July 2016
Accepted 12 July 2016

Keywords:
Iterated function systems
Fractal transformations
Orthogonal expansions
Fourier series

ABSTRACT

Our results and examples show how transformations between self-similar sets may be continuous almost everywhere with respect to measures on the sets and may be used to carry well known notions from analysis and functional analysis, for example flows and spectral analysis, from familiar settings to new ones. The focus of this paper is on a number of surprising applications including what we call fractal Fourier analysis, in which the graphs of the basis functions are Cantor sets, discontinuous at a countable dense set of points, yet have good approximation properties. In a sequel, the focus will be on Lebesgue measure-preserving flows whose wave-fronts are fractals. The key idea is to use fractal transformations to provide unitary transformations between Hilbert spaces defined on attractors of iterated function systems.

1. Introduction

The study of self-similar sets via iterated function systems (IFSs) has been intense for over 30 years. Only recently, however, have fractal transformations between the attractors of two IFSs been investigated [7,8,10]. In this paper, such fractal transformations are used to transform classical notions from analysis and functional analysis on one attractor (say a line segment, a square, or a circle) to a fractal version of these notions on the other - thus the title "old wine in fractal bottles".

One instance of this "rebottling" considered in this paper is to transform Fourier analysis on an interval to a fractal setting. An example is shown in Fig. 1, illustrating two approximations to a piecewise constant function with a jump in the middle. The fractal sine series (red) has a dense set of discontinuities yet makes a clean jump, while the comparable sine series (black) makes no jump, due to the constraint of continuity and the Gibbs effect. The L^2 and L^∞ errors of both approximations are nearly the same, but the distributions of the errors are different.

If $F = \{X;\ f_1, f_2, \ldots, f_N\}$ is a contractive IFS with attractor A and with positive probability vector $p = (p_1, p_2, \ldots, p_N)$, then there is an *invariant measure* μ_p associated with the pair (F, p). According to a theorem of Elton [12], this measure of a Borel set B, whose boundary has measure zero, is, "almost always", in the limit, the proportion of points in the chaos game algorithm that land in B, where the function f_i is chosen in the chaos game with probability p_i for all i.

Let F and G be two contractive IFSs with the same number of functions and with the same probability vector, with non-overlapping (defined in Section 2.2) attractors A_F and A_G and with respective invariant measures μ_F and μ_G. The *fractal transformations* T_{FG}: $A_F \to A_G$ and T_{GF}: $A_G \to A_F$ (defined in Section 2.2) are proved to be measurable and continuous almost everywhere with respect to μ_F and μ_G, respectively. Moreover, these fractal transformations are measure preserving. In some interesting cases, for which a sufficient condition is provided, T_{FG} and T_{GF} are homeomorphisms and inverse to each other.

For an IFS F with attractor A_F, the set L^2_F of complex valued functions on A_F, square integrable with respect to an invariant measure, is a Hilbert space. Given two IFSs with non-overlapping attractors, a fractal transformation T_{FG}: $A_F \to A_G$ induces a transformation from L^2_F to L^2_G. Moreover, the operator $U_{FG} : L^2_F \to L^2_G$ induced by the fractal transformation T_{FG} may be an isometry. Such isometries allow for basic notions and results from analysis and functional analysis to be transferred from the classical setting to a fractal setting. For example, if $A_F = A_G = [0, 1]$, the unit interval, and $\mu_F = \mu_G$ is Lebesgue measure, then U_{FG} takes any orthonormal (ON) basis of functions for $L^2([0, 1])$ to another ON basis for $L^2([0, 1])$. In particular, the standard Fourier ON basis may

* Corresponding author. Tel.: +61 2 61252709; fax: +61 2 6125 4984.
E-mail address: michael.barnsley@anu.edu.au (M. Barnsley).

http://dx.doi.org/10.1016/j.chaos.2016.07.007

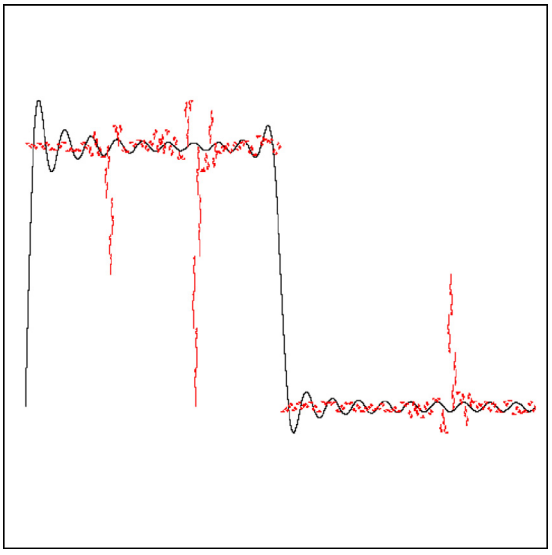

Fig. 1. Partial sums of fractal sine series (red) and a classical sine series (black) both approximate a step function. The fractal series makes a clean jump but pays a price elsewhere. (For interpretation of the references to colour in this figure legend, the reader is referred to the web version of this article.)

be transformed to a "fractal Fourier" ON basis - which leads to fractal Fourier analysis. We note that this kind of spectral analysis is distinct from the analysis on fractals of Kigami [17], Strichartz [27] and others, whereby spectral analysis on some fractals, associated with certain natural Laplacians, is developed *de novo*.

Throughout, except where otherwise stated, we assume that each IFS $F = \{A; f_1, f_2, \dots, f_N\}$ is contractive, and that the ambient space of each IFS is its attractor. We further assume that each function in the IFS is a homeomorphism onto its image, and that F is endowed with a probability vector $p = (p_1, p_1, \dots, p_N)$ with μ_p the associated invariant measure.

The paper is organized as follows. The definitions of the terms above and of other relevant terms are reviewed in Section 2. In particular, in Section 2.2 we recall the definition of the dynamical boundary of an attractor of an IFS, and then define an attractor to be non-overlapping if it is not equal to its dynamical boundary. In Section 2.3 we introduce fractal transformations. In Section 2.4 it is shown that the measure of the critical set (overlap set) and of the dynamical boundary of a non-overlapping attractor of an IFS is zero, for any probability vector. In Section 2.5 it is shown that, given two such IFSs F and G with equal probability vectors and a fractal transformation $T_{FG}: A_F \to A_G$ from the attractor A_F of F to the attractor A_G of G, the fractal transformations T_{FG} and T_{GF} are measurable and continuous almost everywhere with respect to the invariant measures μ_F and μ_G, respectively. Moreover, T_{FG} and T_{GF} are measure preserving in the sense that $\mu_F \circ T_{GF} = \mu_G$ and $\mu_G \circ T_{GF} = \mu_F$.

Examples of fractal transformations which illustrate results of Section 2 appear in Section 3. These include self mappings of the interval, a mapping from the unit interval to a filled triangle and to the Koch curve, a mapping from a filled triangle to itself, and the Hilbert's space filling curve.

Given two IFSs with non-overlapping attractors, with the same number of functions, a fractal transformation T_{FG} acts naturally on the set L^2_F of square integrable complex valued functions on A_F. This provides a map

$$U_{FG} : L^2_F \to L^2_G$$
$$(U_{FG} f)(x) = f(T_{GF} x)$$

for all $f \in L^2_F$ and all $x \in A_F$. Thus, for each ordinary function, there is a fractal version of that function.

The mapping U_{FG} is the subject of Section 4. The main result is that U_{FG} and U_{GF} are isometries and inverses of each other. In the case that $A := A_F = A_G$ and the invariant measures on these spaces are the same, the maps U_{FG} and U_{GF} are unitary transformations with adjoint $U^*_{FG} = U_{GF}$. As a consequence, any classical orthonormal basis for L^2_F (Fourier, Legendre, Haar) can be transformed into ON basis for L^2_G, a fractal version of the original. In the Fourier case, this leads to what we refer to as fractal Fourier analysis. Examples are provided in Section 4.

2. Fractal transformations and invariant measures

This section introduces some essential concepts that run throughout the paper, including (1) the invariant measure of an IFS with probabilities, called a p-measure, and (2) fractal transformations from the attractor of one IFS to the attractor of another. The main results needed in this paper are Theorem 2.2 which states that, if an attractor is not equal to its dynamical boundary, then all p-measures of the critical set, the dynamical boundary, and the inner boundary are zero; and Theorem 2.3 which states that a fractal transformation between non-overlapping attractors is measurable and continuous almost everywhere with respect to every p-measure, and that such a fractal transformation is p-measure preserving.

2.1. Attractors and code space

We recall definitions and basic facts which lead to the central notion of non-overlapping attractor. Let $\mathbb{N} = \{1, 2, 3, \dots\}$ and $\mathbb{N}_0 = \{0, 1, 2, \dots\}$. Throughout this paper we restrict attention to iterated function systems (IFSs) of the form

$$F = \{X; f_1, f_2, \dots, f_N\}$$

where $N \in \mathbb{N}$ is fixed, X is a complete metric space, and $f_i: X \to X$ is a contraction for all $i \in I := \{1, 2, \dots, N\}$. By **contraction** we mean there is $\lambda \in [0, 1)$, such that $d_{\mathbb{X}}(f_i(x), f_i(y)) \le \lambda d_{\mathbb{X}}(x, y)$ for all $x, y \in X$, for all $i \in I$.

For subsets $U \subset X$ let

$$F^{-1}(U) = \bigcup_{i=1}^{N} f_i^{-1}(U) \qquad \text{and} \qquad F(U) = \bigcup_{i=1}^{N} f_i(U).$$

This defines mappings F, F^{-1} on the family 2^X of all subsets of X. Let F^{-k} mean F^{-1} composed with itself k times; let F^k mean F composed with itself k times, for $k \in \mathbb{N}$. Let $F^0 = F^{-0} = I$.

$\mathbb{H}(X)$ will denote the collection of nonempty compact subsets of X. The classical Hutchinson operator $F : \mathbb{H}(X) \to \mathbb{H}(X)$ is just the operator F above restricted to $\mathbb{H}(X)$. According to the basic theory of contractive IFSs as developed in [16], there is a unique **attractor** $A \subset X$ of F. That is, A is the unique nonempty compact subset of X such that

$$A = F(A)\ , \qquad \text{with the property} \quad A = \lim_{k\to\infty} F^k(B)\ ,$$

where convergence is with respect to the Hausdorff metric and is independent of $B \in \mathbb{H}(X)$.

Since, in this paper, we are only interested in A itself, we usually take $X = A$. Throughout this paper the following assumptions are made:

- $F = \{A; f_1, f_2, \dots, f_N\}$ is an IFS with attractor A such that each of its functions is a contraction and is a homeomorphism onto its image.

Note that under this assumption $f_i^{-1} \circ f_i(B) = B$, but $f_i \circ f_i^{-1}(B)$ often differs from B.

Let $I^\infty = \{1, 2, \dots, N\}^\infty$, referred to as the **code space**, be the set of all infinite sequences $\theta = \theta_1\theta_2\theta_3\cdots$ with elements from

I. The **shift operator** S: $I^\infty \to I^\infty$ is defined by $S(\theta_1\theta_2\theta_3\cdots) = \theta_2\theta_3\theta_4\cdots$. Define a metric d on $I^\infty = \{1, 2, \ldots, N\}^\infty$ so that, for θ, $\sigma \in I^\infty$ with $\theta \neq \sigma$, the distance $d(\theta, \sigma) = 2^{-k}$, where k is the least integer such that $\sigma_k \neq \theta_k$. The pair (I^∞, d) is a compact metric space.

Example 2.1 (The code space IFS)**.** Consider the IFS $Z = \{I^\infty; s_1, s_2, \ldots, s_N\}$, where s_i: $I^\infty \to I^\infty$ is defined by $s_i(\sigma) = i\sigma$. The attractor of Z is I^∞; each s_i is a contraction and a homeomorphism onto its image. In particular, a contraction constant is $\lambda = \frac{1}{2}$, independently of i.

Definition 2.1. For any IFS $F = \{A; f_1, f_2, \ldots, f_N\}$, the **coding map** π: $I^\infty \to A$ is defined by

$$\pi(\sigma) = \lim_{k\to\infty} f_{\sigma_1} \circ f_{\sigma_2} \circ \cdots \circ f_{\sigma_k}(a),$$

for a fixed $a \in A$, for all $\sigma = \sigma_1\sigma_2\cdots \in I^\infty$.

Under the assumption that the IFS is contractive, it is well known that the limit is a single point, independent of $a \in A$, convergence is uniform over I^∞, and π is continuous and onto. The sequence σ is called an **address** of the point $x \in A$ if $\pi(\sigma) = x$. The map π is a conjugation between the code space IFS and the given IFS F, in the sense that for all $\sigma \in I^\infty$ and $i = 1, \ldots, N$

$$\pi(s_i(\sigma)) = f_i(\pi(\sigma)) \qquad \text{and} \qquad \pi(S(\sigma)) \in F^{-1}(\pi(\sigma)). \quad (2.1)$$

Thus the code space provides the archetypal IFS, and all other IFS are obtained from Z by an appropriate projection. The map π can be a homeomorphism but usually it will not be one-to-one.

Definition 2.2. For the IFS F, the **critical set** or overlapping set of the attractor A (w.r.t. F) is

$$C = \bigcup_{i\neq j} f_i(A) \cap f_j(A).$$

The **inner boundary** of the attractor A (w.r.t. F) is

$$\widehat{C} = \bigcup_{k\in\mathbb{N}_0} F^k(C)$$

The inner boundary of A is the set of points with more than one address:

$$\widehat{C} = \{x \in A : |\pi^{-1}(x)| \neq 1\}.$$

2.2. The open set condition and non-overlapping attractors

It is necessary in this paper to require that the critical set and inner boundary of an attractor are not too large, so that the pieces generated by the IFS can still be recognized. This is essential since $\widehat{C}$ will be the exceptional set, where a fractal transformation may not be continuous. In the classical case of an IFS consisting of similitudes on $X = \mathbb{R}^n$, P.A.P. Moran [21] noted already in 1945 that open sets can be used to show that C is small, and to construct an appropriate Hausdorff measure on A.

Definition 2.3. The IFS $F = \{X; f_1, f_2, \ldots, f_N\}$ with attractor A fulfils the **open set condition** (OSC) if there exists a nonempty subset O of X, such that $f_i(O) \subset O$ and $f_i(O) \cap f_j(O) = \emptyset$ for $i \neq j$, for all $i, j = 1, 2, \ldots, N$.

Theorem 2.1 ([21], Theorem III, cf. [16], [13], Theorem 9.3)**.** *If $F = \{\mathbb{R}^n; f_1, f_2, \ldots f_N\}$ consists of similitudes with scaling ratio of f_i equal to $s_i < 1$, and F obeys the OSC, then the Hausdorff dimension D of the attractor A is the unique positive solution to $\sum_{i=1}^N s_i^D = 1$. The D-dimensional Hausdorff measure is positive and finite on A. Up to a constant factor, it is the invariant measure μ_p with probabilities $p_i = s_i^D$. (See Definition 2.4.)*

Since the proof uses Lebesgue measure on the open set O, it is important to work on $\mathbb{R}^n$, not only on A itself. The open set condition is often difficult to check although it can be formulated algebraically in terms of the data of the IFS [2]. Schief proved that for similitudes in complete metric spaces, the OSC with $O \cap A \neq \emptyset$ implies the above equation for Hausdorff dimension, while on the other hand, positive finite D-dimensional Hausdorff measure of A yields the OSC [24].

We are interested, not only in similitudes, but also in affine and non-linear mappings. For this reason we use an internal condition on the IFS and its attractor which was introduced by M. Morán [19], see also Kigami [18]. The condition has a geometric flavor and applies to an IFS with arbitrary contractions in a complete metric space. Let $\overline{U}$ denote the closure of $U \subset X$ and U^o the interior. Since A is compact, the closure of $U \subset A$ within A is the same as in any surrounding space X.

Definition 2.4. The **dynamical boundary** of A (w.r.t. F) is

$$\partial A = \overline{\bigcup_{k=1}^{\infty} F^{-k}(C) \cap A}.$$

Define A to be **non-overlapping** (w.r.t. F) if

$$A \neq \partial A. \quad (2.2)$$

The topological boundary of a set U in a surrounding space X is the set $\overline{U} \cap \overline{X \setminus U}$. In particular, the topological boundary of U in U is always empty. The following example shows that in general ∂A differs from the topological boundary of A in A as well as in X.

Example 2.2. Let $F = \{[0, 1]; f_1, f_2\}$ with Euclidean metric. The topological boundary of $[0, 1]$ in $\mathbb{R}$ is $\{0, 1\}$. If $f_1(x) = \frac{1}{2}x$, $f_2(x) = \frac{1}{2}x + \frac{1}{2}$, then the dynamical boundary of the attractor $A = [0, 1]$ is $\partial A = \{0, 1\}$. In this case, by definition, A is non-overlapping. On the other hand, if $f_1(x) = \frac{2}{3}x$, $f_2(x) = \frac{2}{3}x + \frac{1}{3}$, then again $A = [0, 1]$, but $\partial A = [0, 1]$. In this case A is overlapping.

If the OSC holds for an IFS on $\mathbb{R}^n$ with similitudes, the open set can be chosen so that $O \cap A \neq \emptyset$ [23], in which case A is non-overlapping because O cannot intersect ∂A, [19, Theorem 2.3, through the implications iii)⇒i) and i)⇒ii)]. Conversely, it is conjectured that the non-overlapping condition for similitudes on $\mathbb{R}^n$ implies the OSC. The proof of the statement [19, Theorem 2.3, ii)⇒iii)] is wrong and the question is still open, cf. [3].

For similitudes on complete metric spaces, Morán [19, Theorem 2.3] proved that A is non-overlapping if and only if there exists a set $O \subset A$ open in A which fulfils $F(O) \subset O$ and $F(O) \cap C = \emptyset$. Also Kigami [18, p. 15] proved that every open $O \subset A \setminus \partial A$ fulfils an "intrinsic open set condition". For our purposes, it is important to note that inner and dynamical boundary of a non-overlapping attractor are small in a topological sense.

Proposition 2.1 (cf. [19],[17])**.** *For a non-overlapping attractor, the sets $C, \partial A$, and $\widehat{C}$ do not contain interior points with respect to A.*

Proof. If $U \subseteq A$ is open in A, then there is a piece $A_\sigma = f_{\sigma_1}\cdots f_{\sigma_k}(A)$ at some level k in A which is contained in U, and hence $F^{-k}(U) = A$. Thus $U \subseteq C$ would contradict the non-overlapping property. The same argument shows that $U \subseteq \partial A$ is not possible, since the definition of ∂A implies $F^{-k}(\partial A) = \partial A$ for $k = 1, 2, \ldots$ [19]. Now $\widehat{C}$ is a countable union of closed nowhere dense sets of the form $f_{\sigma_1}\cdots f_{\sigma_k}(C)$, and Baire's category theorem shows that $\widehat{C}$ cannot contain an interior point in the compact set A. □

To show below that the inner and dynamical boundaries are also small in a measure-theoretic sense, we state one more property of non-overlapping attractors (cf. [11]). A point $\omega \in I^\infty$ is called **disjunctive** if $\{S^k\omega : k \in \mathbb{N}\}$ is dense in I^∞.

Proposition 2.2. *If a point x in a non-overlapping attractor has a disjunctive address, it can neither belong to the dynamical nor to the inner boundary.*

Proof. If $\pi(\omega) = x$, then $\pi(S^k(\omega)) \in F^{-k}(x)$ by (2.1). So if x is in ∂A, all of $\pi(S^k(\omega))$ belongs to ∂A. If x is in $\widehat{C}$, then $\pi(S^k(\omega))$ will be in C for $k = k_0$ and in ∂A for all $k > k_0$. On the other hand, if ω is disjunctive then the $\pi(S^k(\omega))$ with $k = 1, 2, \dots$ form a dense set in A. Non-overlapping means that ∂A is not dense in A, so ω disjunctive means that $\pi(\omega)$ is not a boundary point. □

2.3. Fractal Transformations

The purpose of this subsection is to define the central notion of a fractal transformation from one attractor to another.

The code space I^∞ is equipped with the lexicographical ordering, so that $\theta > \sigma$ means $\theta \neq \sigma$ and $\theta_k > \sigma_k$ where k is the least index such that $\theta_k \neq \sigma_k$. Here $1 > 2 > 3 \cdots > N-1 > N$.

Definition 2.5. A **section** of the coding map $\pi: I^\infty \to A$ is a map $\tau: A \to I^\infty$ such that $\pi \circ \tau$ is the identity. In other words τ is a map that assigns to each point in A an *address* in the code space. The **top section** of $\pi: I^\infty \to A$ is the map $\tau: A \to I^\infty$ given by

$$\tau(x) = \max \pi^{-1}(x)$$

for all $x \in A$, where the maximum is with respect to the lexicographic ordering. The value $\tau(x)$ is well-defined because $\pi^{-1}(x)$ is a closed subset of I^∞.

The technique of top sections was developed by Barnsley [5], [6, Section 4.11]. The top section is forward shift invariant in the sense that $S(\tau(A)) = \tau(A)$. See [9] for a classification of all sections such that $S(\tau(A)) \subseteq \tau(A)$. For the following definition see [7] and [8].

Definition 2.6. Let A_F and A_G be the attractors, respectively, of IFSs $F = \{A_F; f_1, f_2, \dots, f_N\}$ and $G = \{A_G; g_1, g_2, \dots, g_N\}$ with the same number of functions. The **fractal transformations** $T_{FG}: A_F \to A_G$ and $T_{GF}: A_G \to A_F$ are defined to be

$$T_{FG} = \pi_G \circ \tau_F \qquad \text{and} \qquad T_{GF} = \pi_F \circ \tau_G,$$

where $\tau_F: A_F \to I^\infty$ and $\tau_G: A_G \to I^\infty$ are sections. If T_{FG} is a homeomorphism, then it is called a **fractal homeomorphism**, and in this case $T_{GF} = (T_{FG})^{-1}$. Except where otherwise implied, it is assumed that the top sections are used.

The general notion of a fractal transformation using a shift invariant section is discussed in [9]. The following proposition gives a sufficient condition for when a fractal transformation is continuous and when it is a homeomorphism. When, in our examples, it is claimed that a certain fractal transformation is continuous, it is the condition in this proposition that is readily verified.

Proposition 2.3. *Let the attractor A_F of the IFS F be non-overlapping, and let $P_F = \{\pi_F^{-1}(x) : x \in A_F\}$, which is a partition of the code space I^∞. For two non-overlapping attractors A_F and A_G, a fractal transformation $T_{FG}: A_F \to A_G$ is continuous if P_F is a finer partition than P_G, i.e., for each part S in P_F there is a part T in P_G such that $S \subseteq T$. If $P_F = P_G$, then T_{FG} is a homeomorphism.*

Proof. Once we verify that $\overline{\tau_F(A_F)} = I^\infty$, the proposition follows immediately from [7, Theorem 1]; see [8], for references and subtler results.

To show that $\overline{\tau_F(A_F)} = I^\infty$, let D denote the set of disjunctive sequences in I^∞. By Proposition 2.2 we have $\pi_F(D) \subseteq A_F \setminus \widehat{C}$. Since $A_F \setminus \widehat{C}$ is the set of points having a single address, the coding map is bijective when restricted to this set; therefore,

$$D \subseteq \pi_F^{-1}(A_F \setminus \widehat{C}) = I^\infty \setminus \pi_F^{-1}(\widehat{C}) \subseteq \tau_F(A_F),$$

the last inclusion because unique addresses must lie in $\tau_F(A)$. But it is well known [26] that D is dense in I^∞. Therefore so is $\tau_F(A)$. □

2.4. Invariant Measures on an Attractor

In this subsection we recall the definition of the invariant measures on an IFS with probabilities, also called p-measures, and determine that both the dynamical boundary of a non-overlapping attractor A and the inner boundary of A have measure zero.

Definition 2.7 ([16], cf. [13])**.** Let $p = (p_1, p_2, \dots, p_N)$ satisfy $p_1 + p_2 + \cdots + p_N = 1$ and $p_i > 0$ for $i = 1, 2, \dots, N$. Such a positive N-tuple P will be referred to as a **probability vector**. There is a unique normalized positive Borel measure μ supported on A and invariant under F in the sense that

$$\mu(B) = \sum_{i=1}^{N} p_i \, \mu(f_i^{-1}(B)) \tag{2.3}$$

for all Borel subsets B of X. We call μ the **invariant measure of** F corresponding to the probability vector p and refer to it as the **p-measure** (w.r.t. F). To emphasize the dependence on p, we may write μ_p in place of μ.

Example 2.3. This is a continuation of Example 2.1, where $Z = \{I^\infty; s_1, s_2, \dots, s_N\}$. For a probability vector $p = (p_1, p_2, \dots, p_N)$, the corresponding p-measure is the Bernoulli measure ν_p where

$$\nu_p([\sigma_1 \sigma_2 \cdots \sigma_n]) = \prod_{i=1}^{n} p_{\sigma_i},$$

where $[\sigma_1 \sigma_2 \cdots \sigma_n] := \{\omega \in I^\infty: \omega_i = \sigma_i \text{ for } i = 1, 2, .., N\}$ denotes a cylinder set, the collection of which generate the sigma algebra of Borel sets of I^∞.

The Bernoulli product measures are the archetypes of self-similar measures:

Proposition 2.4 (Hutchinson [16])**.** *If F is an IFS with probability vector p, corresponding invariant measure μ_p, and Z is the IFS of Example 2.3 with the same probability vector p and corresponding invariant measure ν_p, then $\mu_p(B) = \nu_p(\pi^{-1}(B))$ for all Borel sets B.*

We can now prove that dynamical and inner boundary of a non-overlapping attractor are small in a measure-theoretic sense. They are zero sets with respect to all invariant measures. This was stated by Graf [14, 3.4] and Morán and Rey [20, Theorem 2.1] for similitudes with the OSC on $\mathbb{R}^n$, by Patzschke in [22, Lemma 4.2] for self-conformal sets with the OSC on a Riemannian manifold, and by Kigami [18, Theorem 1.2.4] in a more abstract setting. Disjunctive sequences provide a simple proof for contractions on complete metric spaces.

Theorem 2.2. *For a non-overlapping IFS, the sets $C, \partial A$, and $\widehat{C}$ have measure zero with respect to all invariant measures μ_p on A.*

Proof. For a probability vector p, let ν_p the Bernoulli measure on I^∞, as above. Let $D \subset I^\infty$ be the set of disjunctive sequences. It is not difficult to prove that $\nu_p(D) = 1$ for all probability vectors p, see [26].

Proposition 2.2 says that $A \setminus \partial A$ contains all points with disjunctive addresses. That is, $\pi^{-1}(A \setminus \partial A) \supseteq D$. Proposition 2.4 implies

$$\mu_p(A \setminus \partial A) = \nu_p(\pi^{-1}(A \setminus \partial A)) \geq \nu_p(D) = 1\,.$$

Since μ_p is a probability measure, $\mu_p(A \setminus \partial A) = 1$ and $\mu_p(\partial A) = 0$. The set C fulfils $f_i^{-1}(C) \subset \partial A$ for $i = 1, \dots, N$. So (2.3) yields $\mu_p(C) = 0$. The same argument is used to show that $\mu_p(F(C)) = 0$, and, inductively, $\mu_p(F^k(C)) = 0$ for $k = 2, 3, \dots$ Thus $\mu_p(\widehat{C}) = 0$. □

Remark. Let F and G be two IFSs with the same number of functions and with A_F non-overlapping. If T_{FG} and T'_{FG} are two fractal transformations from attractor A_F to attractor A_G corresponding to two sections, then $T_{FG} = T'_{FG}$ almost everywhere with respect

to any invariant measure on A_F, i.e., corresponding to any probability vector p for F. More specifically, $T_{FG}(x) = T'_{FG}(x)$ for all x except those x in the set $\widehat{C}_F$ of measure zero. This follows from Theorem 2.2 because, if τ_F and τ'_F are the sections used to form T_{FG} and T'_{FG}, respectively, then τ_F and τ'_F agree everywhere except on $\widehat{C}_F$.

2.5. Continuity and Measure Preserving Properties of Fractal Transformations

The main results of this subsection are that fractal transformations between non-overlapping attractors are measurable, continuous almost everywhere, and map p-measures to p-measures.

Theorem 2.3 ([6], Theorem 4.11.5)**.** *Let $F = \{A; f_1, f_2, \dots, f_N\}$ be an IFS with non-overlapping attractor A, probability vector p, and corresponding invariant measure μ. The section $\tau: A \to I^\infty$ is measurable and continuous almost everywhere w.r.t. μ_p, for all p.*

Proof. The function τ is measurable because $\tau^{-1}[\sigma_1 \dots \sigma_n]$ (cf. Example 2.3) is a Borel set in A which is easily determined by a recursive procedure [6, Section 4.11]. The proof given in [6] can be simplified as follows. Since $\widehat{C}$, the set of points with multiple addresses, has μ_p measure zero, it is enough to show that the bijective map $\tau : A \setminus \widehat{C} \to I^\infty$ is continuous. Take a sequence with limit $x_n \to x$ in $A \setminus \widehat{C}$, and let σ be an accumulation point of $\tau(x_n)$ which by compactness exists. Since π is continuous, we must have $x_n = \pi(\tau(x_n)) \to \pi(\sigma) = x$, by uniqueness of the limit. Thus $\tau(x) = \sigma$, and this is the only accumulation point. The restricted τ is continuous. □

For an IFS F, let

$$\Gamma_F = \pi_F^{-1}(\widehat{C}_F).$$

Consider two non-overlapping IFSs F and G with the same probability vector. With notation as in Definition 2.6 of fractal transformation, let

$$\Gamma_{\{F,G\}} = \Gamma_F \cup \Gamma_G \quad \text{and} \quad \Lambda_{\{F,G\}} = I^\infty \setminus \Gamma_{\{F,G\}}$$
$$A_F^1 = \pi_F(\Lambda_{\{F,G\}}) \quad \text{and} \quad A_G^1 = \pi_G(\Lambda_{\{F,G\}})$$
$$A_F^0 = A_F \setminus A_F^1 \quad \text{and} \quad A_G^0 = A_G \setminus A_G^1$$

Note that A_F^0 depends also on G and that A_G^0 depends also on F; similarly for A_F^1 and A_G^1.

Proposition 2.5. *Assume that both A_F and A_G are non-overlapping, and let μ_F and μ_G be invariant measures associated with the same probability vector. With notation as above*

1. $\mu_F(A_F^1) = \mu_G(A_G^1) = 1$,
2. *The fractal transformation T_{FG} maps A_F^1 bijectively onto A_G^1, and maps A_F^0 into A_G^0.*
3. *Restricted to A_F^1 we have $(T_{FG})^{-1} = T_{GF}$; hence $(T_{FG})^{-1} = T_{GF}$ almost everywhere.*

Proof. Using Proposition 2.4 and Theorem 2.2 we have $\nu(\Gamma_F) = \nu(\pi_F^{-1}\widehat{C}_F) = \mu_F(\widehat{C}_F) = 0$. This implies that $\nu(\Gamma_{\{F,G\}}) = 0$ or $\nu(\Lambda_{\{F,G\}}) = 1$. Again using Proposition 2.4 we have $\mu_F(A_F^1) = \mu_F(\pi_F(\Lambda_{\{F,G\}})) = \nu(\pi_F^{-1}\pi_F(\Lambda_{\{F,G\}})) \geq \nu(\Lambda_{\{F,G\}}) = 1$. This proves statement (1).

Concerning statement (2), we know that $\pi_F^{-1} = \tau_F$ is single-valued on $A_F \setminus \widehat{C}_F \supset A_F^1$. Now τ_F takes A_F^1 bijectively onto $\Lambda_{\{F,G\}}$ and π_G takes $\Lambda_{\{F,G\}}$ bijectively onto A_G^1. Similarly, τ_F takes A_F^0 into $\Gamma_{\{F,G\}}$ and π_G takes $\Gamma_{\{F,G\}}$ into A_G^0.

Concerning statement (3), restricted to A_G^1 we have $T_{FG} \circ T_{GF} = \pi_G \circ (\tau_F \circ \pi_F) \circ \tau_G = \pi_G \circ \tau_G = I$, the identity. □

Theorem 2.4. *Assume that both A_F and A_G are non-overlapping, and let μ_F and μ_G be invariant measures associated with the same probability vector. Then*

1. *$T_{FG}: A_F \to A_G$ is measurable and continuous a.e. with respect to μ_F;*
2. *$\mu_F \circ T_{GF} = \mu_G$ and $\mu_G \circ T_{FG} = \mu_F$.*

Proof. Since $T_{FG} = \pi_G \circ \tau_F$, statement (1) follows from the continuity of $\pi_G: I^\infty \to A_G$ and Theorem 2.3.

Concerning statement (2), let B be a Borel set in A_G, and let $B^0 = B \cap A_G^0$, $B^1 = B \cap A_G^1$. By Propositions 2.4 and 2.5

$$\begin{aligned}\mu_G(B) &= \mu(\pi_G^{-1}B) = \mu(\pi_G^{-1}(B^0 \cup B^1)) \\ &= \mu(\pi_G^{-1}B^0) + \mu(\pi_G^{-1}B^1) = \mu(\tau_G B^1),\end{aligned}$$

the last equality because $\pi_G^{-1}(B^0) = \tau_G(B^0)$, which has measure zero.

By similar arguments

$$\begin{aligned}\mu_F(T_{GF}B) &= \mu_F(T_{GF}(B^0 \cup B^1)) = \mu_F(T_{GF}B^0) + \mu_F(T_{GF}B^1) \\ &= \mu(\pi_F^{-1} \circ \pi_F \circ \tau_G(B^1)) = \mu(\tau_G B_1),\end{aligned}$$

the second to last equality because $T_{GF}(B^0) \subset A_F^0$, which has measure zero. □

For the special case of similitudes in $\mathbb{R}^n$ with the OSC, we obtain a correspondence between the normalized Hausdorff measures of Theorem 2.1.

Proposition 2.6. *Let $F = \{A_F \subset \mathbb{R}^n; f_1, f_2, \dots f_N\}$ and $G = \{A_G \subset \mathbb{R}^n; g_1, g_2, \dots g_N\}$ be two IFS satisfying the open set condition and consisting of similitudes with scaling ratios s_i, $t_i < 1$ respectively. If $s_i^{D_F} = t_i^{D_G}$ for all i, then*

$$\mu_F = \mu_G \circ T_{FG},$$

where μ_F and μ_G are the normalized D_F and D_G-dimensional Hausdorff measures on A_F and A_G, respectively, where the probabilities are $p_i = s_i^{D_F} = t_i^{D_G}$.

3. Examples

Example 3.1 (Fractal homeomorphisms of an interval)**.** Consider IFSs $F = \{([0, 1]; f_1, f_2\}$ and $G = \{([0, 1]; g_1, g_2\}$, with probabilities p_1, p_2, where

$$f_1(x) = p_1 x, \quad f_2(x) = p_2 x + p_1$$
$$g_1(x) = r x, \quad g_2(x) = (1 - r)x + r,$$

and $0 < r < 1$. The OSC is fulfilled and we have only one critical point $C_F = \{p_1\}$, $C_G = \{r\}$, with addresses $1\overline{2}$ and $2\overline{1}$ in both cases. Thus the fractal transformation $T_{FG} : [0, 1] \to [0, 1]$ is a homeomorphism by Proposition 2.3. By Theorem 2.1, the invariant measure for F is Lebesgue measure λ while G describes an arbitrary p-measure μ_p. By Theorem 2.4, T_{FG} transforms λ to μ_p and T_{GF} transforms μ_p to λ. This example can be generalized from 2 to N functions.

Thus each p-measure of such an IFS can be transformed to Lebesgue measure by a fractal homeomorphism. It is well known that each non-atomic probability measure μ on $[0, 1]$ can be transformed into λ by a homeomorphism F, which is in fact the cumulative distribution function of μ. In the case of a fractal homeomorphism, the piece structure is also preserved. This may be useful for Haar wavelets, as indicated in Section 4.

The next two examples deal with the special case of the binary representation of [0, 1],

$$F = \left\{[0, 1];\ f_1 = \frac{x}{2},\ f_2 = \frac{x}{2} + \frac{1}{2}\right\}, \quad p_1 = p_2 = \frac{1}{2}\ .$$

Example 3.2 (The Cantor function)**.** Consider the IFS $G = \{\mathcal{C};\ \frac{1}{3}x, \frac{1}{3}x + \frac{2}{3}\}$ with attractor equal to the standard Cantor set $\mathcal{C}$

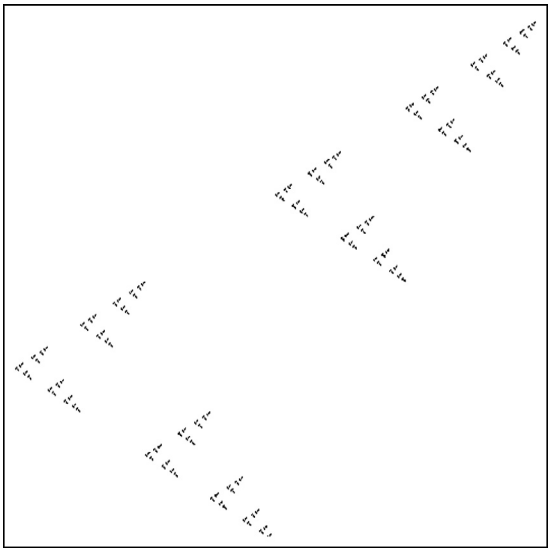

Fig. 2. Graph of the fractal transformation T_{FG_1} discussed in Example 3.3. The transformation preserves Lebesgue measure on [0,1] and is continuous except for a dense countable set of discontinuities. The viewing window is slightly larger than [0,1] × [0,1].

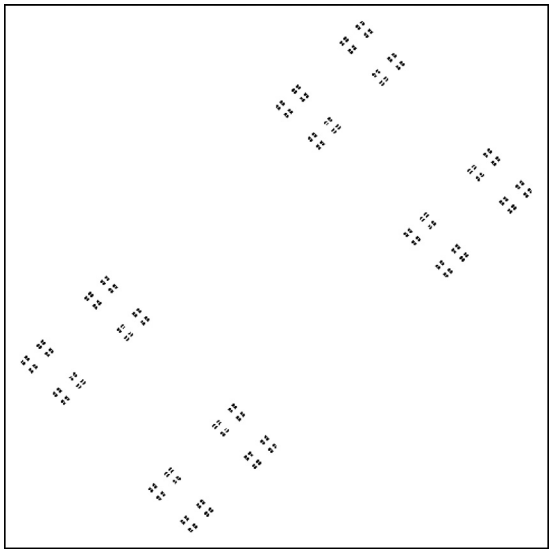

Fig. 3. Graph of the fractal transformation T_{FG_2} discussed in Section 3.3. Unlike T_{FG_1} in Fig. 2, T_{FG_2} is its own inverse.

and empty critical set, while the attractor of F is $[0, 1]$ and the critical set is $\{\frac{1}{2}\}$. In this case $T_{GF} : \mathcal{C} \to [0, 1]$ is continuous and essentially the Cantor function, called "devil's staircase" by Mandelbrot. The Cantor function is usually defined as a function $f : [0, 1] \to [0, 1]$ so that if x is expressed in ternary notation as $x = i_1\, i_2 \cdots$ where $i_k \in \{0, 1, 2\}$ for all k, then $f(x) = i'_1\, i'_2 \cdots$ expressed in binary, where $i' = 0$ if $i \in \{0, 1\}$ and $i' = 1$ if $i = 2$. The function $T_{GF} : \mathcal{C} \to [0, 1]$ is the restriction of this function to $\mathcal{C}$ where $i_k = 1$ is forbidden. The inverse $T_{FG} : [0, 1] \to \mathcal{C}$ is discontinuous at $\frac{1}{2}$ and points of the form $k/2^n$.

Example 3.3 (Self mappings of the interval)**.** Beside F, there are three other IFSs which fulfil the OSC and have the Lebesgue measure as invariant measure for $p_1 = p_2 = \frac{1}{2}$.

$$G_1 = \left\{[0, 1];\ g_1 = -\frac{x}{2} + \frac{1}{2},\ g_2 = \frac{x}{2} + \frac{1}{2}\right\},$$

$$G_2 = \left\{[0, 1];\ g_1 = -\frac{x}{2} + \frac{1}{2},\ g_2 = -\frac{x}{2} + 1\right\},$$

$$G_3 = \left\{[0, 1];\ g_1 = \frac{x}{2},\ g_2 = -\frac{x}{2} + 1\right\}.$$

Thus $A_F = A_{G_i} = [0, 1]$ for $i = 1, 2, 3$. All four IFSs have the critical set $C = \{\frac{1}{2}\}$ and the inner boundary

$$\widehat{C} = \left\{\frac{k}{2^n} : k = 0, 1, \ldots, 2^n; n \in \mathbb{N}\right\}.$$

The three fractal transformations T_{FG_i}, $i = 1, 2, 3$, are homeomorphism when restricted to $[0, 1]\backslash\widehat{C}$. Due to the choice of the top section, the T_{FG_i} are continuous from the left at all points in $(0, 1]$. For $p_1 = p_2 = \frac{1}{2}$, the p-measure is Lebesgue measure on $[0, 1]$, which is preserved by the T_{FG_i} according to Proposition 2.6. The graph of the function T_{FG_1} appears in Fig. 2, and the graph of T_{FG_2} appears in Fig. 3.

The fractal transformation T_{FG_2} is its own inverse, i.e., $T_{FG_2} \circ T_{FG_2} = id$, the identity, a.e. This can be verified using binary representation:

$$x = \sum_{n=1}^{\infty} d_n/2^n,\quad d_n \in \{0, 1\},\quad \text{implies}\quad T_{FG_2}(x) = \sum_{n=1}^{\infty} (-1)^{n-1}\, d_n/2^n.$$

Example 3.4 (Koch curves and space-filling curves)**.** For the IFS G_2 above, which we call G now, the two addresses of the critical point $\frac{1}{2}$ are $1\overline{12}$ and $2\overline{21}$. Exactly the same identification of addresses can be obtained in the complex plane when we replace the factor -0.5 by $-0.5 \pm \alpha i$ with $-0.5 < \alpha < 0.5$. The attractor A_G of

$$F = F_\alpha = \{\mathbb{C};\ f_1 = (-0.5 - \alpha i)z,\ f_2 = (-0.5 + \alpha i)z + 1.5 - \alpha i\}$$

is a fractal curve. See [4, Figures VIII.237 and VIII.238] where other constant terms were used. (Here we defined F so that the fixed points of f_1, f_2 are 0 and 1 but the endpoints of the curve are the fixed points of $f_1 f_2$ and $f_2 f_1$.) The OSC is easy to verify. For $\alpha = \sqrt{3}/6$ the mappings involve a rotation around $\pm\ 150^o$, so we obtain the classical Koch snowflake curve. Since C_α is always a single point with addresses $1\overline{12}$ and $2\overline{21}$, the fractal transformations T_{GF}, T_{FG} are homeomorphisms between interval and Koch curve with $T_{FG} = T_{GF}^{-1}$, by Proposition 2.3.

For $p_1 = p_2 = 0.5$, the measure μ_G is Lebesgue measure on $[0, 1]$. The pushfoward of μ_G to A_F under T_{GF} is the normalized Hausdorff measure μ_F on the Koch curve A_F, by Proposition 2.6. (We remark that the measure of any Borel subset B of A_F may be computed by, and thought of in terms of the chaos game algorithm on F with equal probabilities, [12].) The Hausdorff dimensions of A_G and A_F are 1 and $\ln 2/\ln 1/r$, where $r = \sqrt{\frac{1}{4} + \alpha^2}$ is the ratio of f_1 and f_2. Thus, a fractal transformation may change the dimension of a set upon which it acts.

Now consider the case $\alpha = \frac{1}{2}$. The mappings f_1, f_2 involve a rotation around $\pm\ 135^o$, and the attractor $A_F = \blacktriangle$ becomes a right-angled isosceles triangle, with dimension $\ln 2/\ln 1/r$ equal to 2. The OSC is still fulfilled, the addresses $1\overline{12}$ and $2\overline{21}$ are still identified. However, many new identifications arise. The critical set is an interval - the altitude of $\blacktriangle$ is the intersection of the pieces $f_1(\blacktriangle)$ and $f_2(\blacktriangle)$. According to Proposition 2.3 the transformation T_{GF} remains continuous, and describes a plane-filling curve. For $p_1 = p_2 = 0.5$ the one-dimensional Lebesgue measure μ_G on $[0, 1]$ is transformed into the two-dimensional Lebesgue measure μ_F on $\blacktriangle$. Moreover, $T_{GF} : \blacktriangle \to [0, 1]$ is continuous almost everywhere with respect to two-dimensional Lebesgue measure, with discontinuities located on a countable set of intervals. We have that $T_{GF} \circ T_{FG}(x) = x$ for all $x \in \blacktriangle$, and $T_{FG} \circ T_{GF}(x) = x$ for almost all $x \in [0, 1]$, with respect to one-dimensional Lebesgue measure. $T_{FG}(\blacktriangle)$ is not the whole interval $[0, 1]$ but a dense subset of $[0, 1]$.

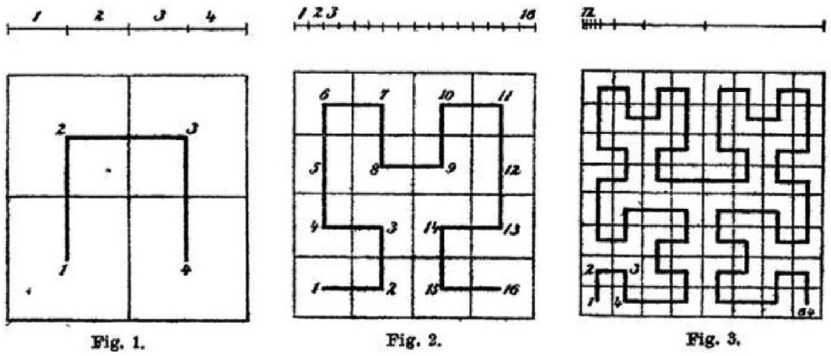

Fig. 4. Hilbert's original design for a continuous map from [0,1] to [0,1] × [0,1].

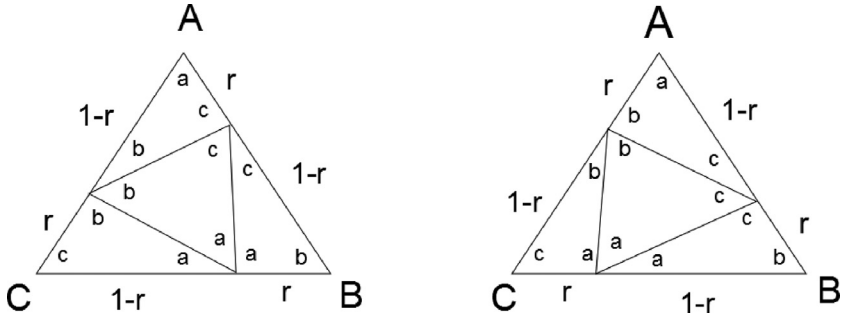

Fig. 5. See Example 3.6.

Example 3.5 (Hilbert's space filling curve)**.** Space filling curves, from the point of view of IFS theory, have been considered in [25]. In [7] it is shown how, as follows, functions such as the Hilbert mapping h: $[0, 1] \to [0, 1]^2$ (see Fig. 4) are examples of fractal transformations.

Let $A = A_1 = (0, 0), B = B_2 = (0, 1), C = C_3 = (1, 1), D = D_4 = (1, 0)$, $D_1 = A_2 = (0, 0.5)$, $C_1 = D_2 = A_3 = B_4 = (0.5, 0.5)$, $B_1 = C_4 = (0.5, 0), C_2 = B_3 = (0.5, 1)$, and $D_3 = A_4 = (1, 0.5)$. Let

$$F = \left\{\mathbb{R}; f_i = \frac{x + i - 1}{4}, i = 1, 2, 3, 4\right\},$$

$$G = \left\{\mathbb{R}^2; g_i, i = 1, 2, 3, 4\right\}$$

where $g_i : \mathbb{R}^2 \to \mathbb{R}^2$ is the unique affine transformation such that $g_i(ABCD) = A_iB_iC_iD_i$, by which we mean $g_i(A) = A_i$, $g_i(B) = B_i, g_i(C) = C_i, g_i(D) = D_i$ for $i = 1, 2, 3, 4$. (Similar notation will be used elsewhere in this paper.) In complex notation, we have the explicit expressions

$$g_1(z) = \frac{i\bar{z}}{2}, g_2(z) = \frac{(z + i)}{2}, g_3(z) = \frac{(z + 1 + i)}{2},$$

$$g_4(z) = \frac{(-i\bar{z} + 2 + i)}{2}.$$

The Hilbert mapping is $h = T_{FG} : [0, 1] \to [0, 1]^2$. The functions in G were chosen to conform to the orientations of Fig. 4, which comes from Hilbert's paper [15] concerning Peano curves. That T_{FG} is continuous follows from Proposition 2.3.

If $p_1 = p_2 = p_3 = p_4 = 0.25$, then, by Proposition 2.1 , the associated invariant measure μ_F is the Lebesgue measure on $[0, 1]$, and μ_G is Lebesgue measure on $[0, 1]^2$. The inverse of T_{FG}^{-1} is the fractal transformation $T_{GF} : [0, 1]^2 \to [0, 1]$, which is continuous almost everywhere with respect to two dimensional Lebesgue measure. More precisely, $T_{GF} \circ h(x) = x$ for almost all $x \in [0, 1]$ (with respect to Lebesgue measure), and $h \circ T_{GF}(x) = x$ for all $x \in [0, 1]^2$. If $0 \le \alpha < \beta \le 1$, then by Proposition 2.1

$$\lambda(h([\alpha, \beta])) = \beta - \alpha,$$

where λ is 2-dimensional Lebesgue measure.

Example 3.6 (A family of fractal homeomorphisms of an equilateral triangle)**.** Let ▲ denote a filled equilateral triangle as illustrated in Fig. 5. The IFS F_r, $0 < r \le \frac{1}{2}$, on ▲ consists of the four affine functions as illustrated in the figure on the left, where ▲ is mapped to the four smaller triangles so that points A, B, C are mapped, respectively, to points a, b, c. A probability vector is associated with F such that the probability is proportional to the area of the corresponding triangle. The IFS G_r is defined in exactly the same way, but according to the figure on the right. The attractor of each IFS is ▲. (Although subtle, there exists a metric, equivalent to the Euclidean metric on $\mathbb{R}^2$, such that both IFSs are contractive, see [1].) Because the functions in F_r and G_r are affine functions rather than similitudes, Theorem 2.1 does not hold. Nevertheless, the corresponding invariant measures μ_F and μ_G are both 2-dimensional Lebesgue measure, because the invariant measure is unique and Lebesgue measure satisfies the defining Eq. (2.3). By Proposition 2.3 and Theorem 2.4, the fractal transformation T_{FG}^r is an area-preserving homeomorphism of ▲ for all $0 < r \le \frac{1}{2}$. This example seems to be the simplest example of an area preserving fractal homeomorphism in $\mathbb{R}^2$.

4. Isometries between Hilbert Spaces

Given an IFS F with attractor A_F and an invariant measure μ_F, the Hilbert space $L_F^2 = L^2(A_F, \mu_F)$ of complex-valued functions on A_F that are square integrable w.r.t. μ_F are endowed with the inner product $\langle \cdot, \cdot \rangle_F$ defined by

$$\langle \psi_F, \varphi_F \rangle_F = \int_{A_F} \overline{\psi_F} \varphi_F \, d\mu_F,$$

for all $\psi_F, \varphi_F \in L_F^2$. Functions that are *equivalent*, i.e., equal almost everywhere, are considered to be the same function in L_F^2.

Definition 4.1. Given two IFSs F and G with the same number of functions, with the same probabilities, with attractors A_F and A_G

and invariant measures μ_F and μ_G, respectively, let T_{FG} and T_{GF} be the fractal transformations. The **induced isometries** $U_{FG} : L^2_F \to L^2_G$ and $U_{GF} : L^2_G \to L^2_F$ are given by

$$(U_{FG}\varphi_F)(y) = \varphi_F(T_{GF}(y))$$
$$(U_{GF}\varphi_G)(x) = \varphi_G(T_{FG}(x))$$

for all $\varphi_F \in L^2_F$ and all $\psi_F \in L^2_G$, for all $x \in A_F$ and all $y \in A_G$. That these linear operators are indeed isometries is proved as part of Theorem 4.1 below.

Theorem 4.1. *Under the conditions of Definition 4.1,*

1. $U_{FG} : L^2_F \to L^2_G$ *and* $U_{GF} : L^2_G \to L^2_F$ *are isometries;*
2. $U_{FG} \circ U_{GF} = id_F$ *and* $U_{GF} \circ U_{FG} = id_G$, *the identity maps on* L^2_F *and* L^2_G *respectively;*
3. $\langle \psi_G, U_{FG}\varphi_F \rangle_G = \langle U_{GF}\psi_G, \varphi_F \rangle_F$ *for all* $\psi_G \in L^2_G$, $\varphi_F \in L^2_F$.

Proof. (1) To show that the linear operators are isometries:

$$\begin{aligned}\|U_{FG}\varphi_F\|^2_G &= \int_{A_G} |U_{FG}\varphi_F|^2 d\mu_G \\ &= \int_{A_G} |\varphi_F \circ T_{GF}|^2 d\mu_G \\ &= \int_{A_F} |\varphi_F|^2 d(\mu_G \circ T_{FG}) \\ &= \int_{A_F} |\varphi_F|^2 d\mu_F = \|\varphi_F\|^2_F,\end{aligned}$$

the third equality from the change of variable formula and Proposition 2.5, the fourth equality from statement (2) of Theorem 2.4.

(2) From the definition of the induced isometries

$$(U_{GF}\, U_{FG}(\varphi_F))(x) = \varphi_F(T_{GF}\, T_{FG}(x)).$$

But by Proposition 2.5, the fractal transformations T_{GF} and T_{FG} are inverses of each other almost everywhere. Therefore the functions $U_{GF}\, U_{FG}(\varphi_F)$ and φ_F are equal for almost all $x \in A_F$.

(3) This is an exercise in change of variables, similar to the proof of (1). □

Let F and G be IFSs with the same number of functions, the same probability vectors, and corresponding invariant measures μ_F and μ_G. If $\{e_n\}$ is an orthonormal basis for L^2_F, then by Theorem 4.1, the set $\{\widehat{e}_n\} = \{U_{FG}\, e_n\}$ is an orthonormal basis for L^2_G. For example, if IFSs F and G have the same attractor $A_F = A_G = [0, 1]$, and the invariant measures are both Lebesgue measure, then the Fourier orthonormal basis $\{e^{2\pi i n x}\}_{n=-\infty}^{\infty}$ of $L^2([0, 1])$ is transformed under U_{FG} to a "fractalized" orthonormal basis of $L^2([0, 1])$. Therefore, every function in $L^2([0, 1])$ has, not only a Fourier series, but also a corresponding (via T_{FG}) fractal Fourier series.

4.1. Fractal Fourier sine series

Consider the IFSs F, G_1, G_2 of Example 3.3 with probabilities $p_1 = p_2 = 0.5$. In this case μ_F, μ_{G_1} and μ_{G_2} are all Lebesgue measure on [0, 1]. Consider the orthonormal Fourier sine basis $\{\sqrt{2}\, e_n\}_{n=1}^{\infty}$ for $L^2[0, 1]$, where $e_n = \sin(n\pi x)$. For the fractal transformations T_{FG_i}, $i = 1, 2$, the fractally transformed orthonormal bases for $L^2[0, 1]$ are $\{\sqrt{2}\,\widehat{e}_n\}_{n=1}^{\infty}$ and $\{\sqrt{2}\,\widetilde{e}_n\}_{n=1}^{\infty}$, where

$$\widehat{e}_n(x) := \sin(n\pi\, T_{G_1F}(x)),$$
$$\widetilde{e}_n(x) := \sin(n\pi\, T_{G_2F}(x))$$

for all $n \in \mathbb{N}$. Fig. 7 illustrates $\widehat{e}_n$, $n = 1, 2, 3$, in colors black, red, and green, respectively. For comparison, Fig. 6 illustrates the corresponding sine functions $e_n = \sin(n\pi x)$ for $n = 1, 2, 3$.

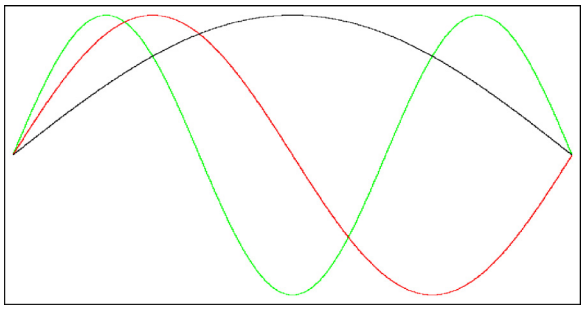

Fig. 6. The sine functions $e_n = sin(n\pi x)$ for n = 1, 2, 3, for comparison with the fractal sine functions shown in Fig. 7.

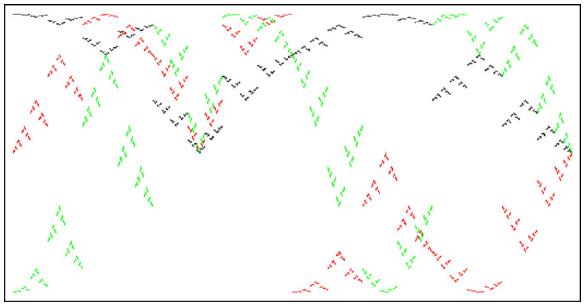

Fig. 7. The fractally transformed sine functions, $\widehat{e}_n = \sin(n\pi T_{G_1F}(x))$, $n = 1$ (black), 2 (red), 3 (green). The viewing window is [0,1] × [-1,1]. (For interpretation of the references to colour in this figure legend, the reader is referred to the web version of this article.)

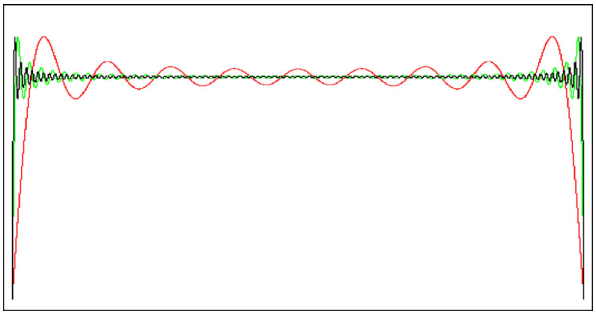

Fig. 8. For comparison with Fig. 9, this shows the Fourier sine series approximations to a constant function on [0, 1] using $k = 10$ (red), 50 (green) and 100 (black) significant terms. Note the well-known end effects at the edges of the interval. (For interpretation of the references to colour in this figure legend, the reader is referred to the web version of this article.)

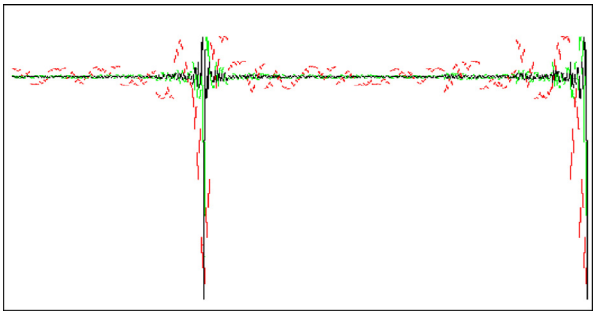

Fig. 9. Fractal sine series approximations to a constant function on the interval [0, 1]. The number of terms used here are 10 (red), 50 (green) and 100 (black). Compare with Fig. 8. The r.m.s. errors are the same as for the approximation to the same constant function using a sine series with the same number of terms. Notice that the edge effect has been shifted from 0 to 1/3. (For interpretation of the references to colour in this figure legend, the reader is referred to the web version of this article.)

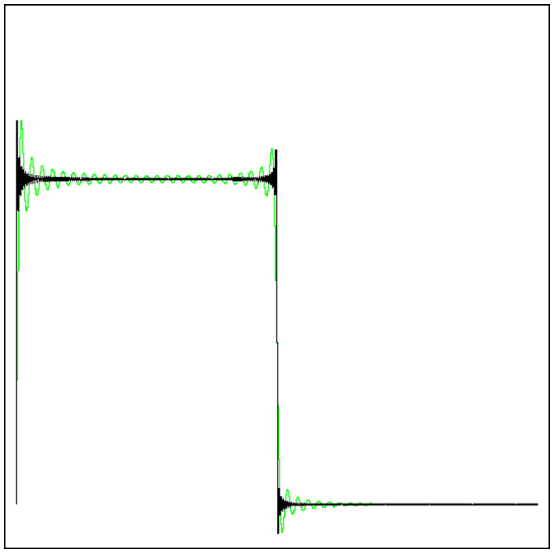

Fig. 10. Sum of the first 100 (green) and 500 (black) terms in the Fourier sine series for a step function. The viewing window is [0,1] × [-0.1,1.5]. Compare with Figs. 11 and 12. (For interpretation of the references to colour in this figure legend, the reader is referred to the web version of this article.)

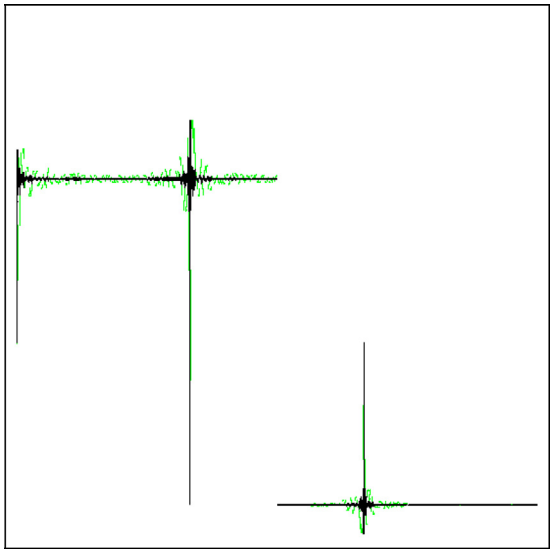

Fig. 11. Sum of the first 100 (green) and 500 (black) terms in a fractal Fourier sine series (using $\widehat{e}_n$ functions) for a step function. Compare with Figs. 10 and 12. (For interpretation of the references to colour in this figure legend, the reader is referred to the web version of this article.)

Example 4.1 (Constant function)**.** Fig. 8 illustrates the standard sine series Fourier approximation to a constant function on the interval [0, 1]. Fig. 9 illustrates three fractal Fourier sine series approximations. The respective Fourier series are

$$\sum_{n=1}^{\infty} \frac{e_{2n-1}(x)}{2n-1} \quad \text{and} \quad \sum_{n=1}^{\infty} \frac{\widehat{e}_{2n-1}(x)}{2n-1}.$$

The calculation, in the fractal case, of the Fourier coefficients, uses the change of variables formula, the fact from Example 3.3 that μ_F and μ_G are Lebesgue measure, and statement 2 of Theorem 2.4.

Example 4.2 (Step function)**.** Figs. 10–12 illustrate the Fourier approximations of a step function for 100 (green) and 500 (black) terms, where the orthogonal basis functions are e_n, $\widehat{e}_n$ and $\widetilde{e}_n$, respectively. The respective Fourier series are

$$\frac{2}{\pi} \sum_{n=1}^{\infty} \frac{1-\cos(n\pi/2)}{n} f_n(x),$$

where f_n is e_n, $\widehat{e}_n$ and $\widetilde{e}_n$, respectively. Note that the jump in the step function at $x = 0.5$ is cleanly approximated in both the fractal series, in contrast to the well-known edge effect (Gibbs phenomenon) in the classical case. The price that is paid is that the fractal approximants have greater pointwise errors at some other values of x in [0, 1]. The analysis of where this occurs and proof that the mean square error is the same for all three schemes, is omitted here.

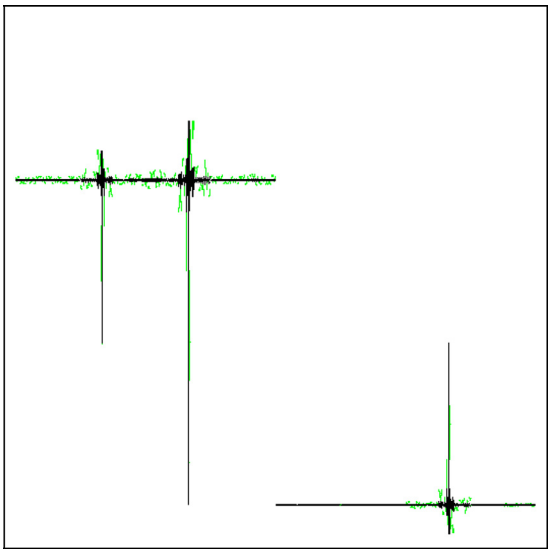

Fig. 12. Sum of the first 100 (green) and 500 (black) terms in a fractal Fourier sine series (using $\widetilde{e}_n$ functions) for a step function. Compare with Figs. 10 and 11. (For interpretation of the references to colour in this figure legend, the reader is referred to the web version of this article.)

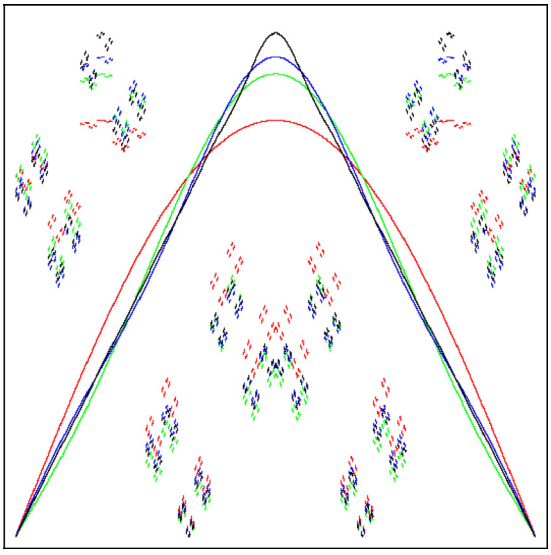

Fig. 13. See Example 4.3. Fourier sine series approximants to a tent function and fractal counterparts.

Example 4.3 (Tent function)**.** In Fig. 13 partial sums of the Fourier sine series and their fractal counterparts are compared, for the tent function $f(x) = \min\{x, 1-x\}$ on the unit interval. The figure shows Fourier approximations to the tent function using orthogonal functions e_n, and fractal approximations to the fractally transformed

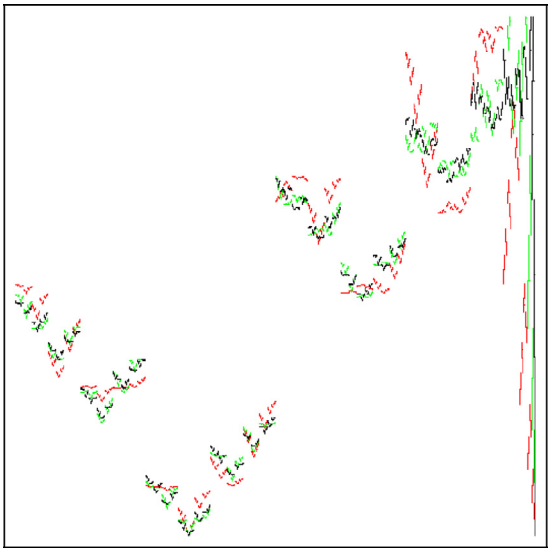

Fig. 14. See Example 4.4. The approximants converge to $T_{G_1F}(x)$ in $\mathcal{L}^2[0,1]$ as the number of terms in series approaches infinity.

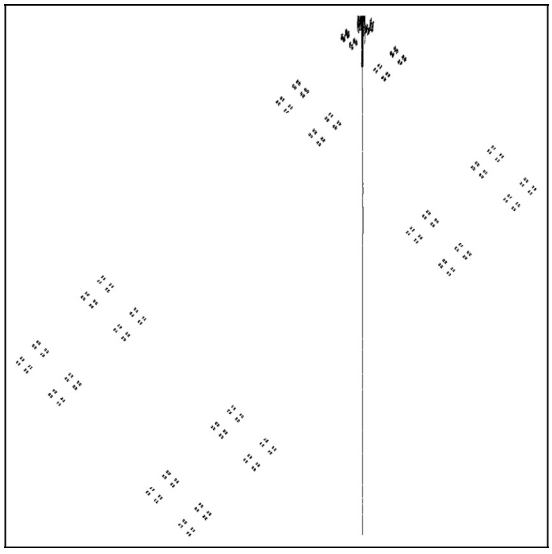

Fig. 15. See Example 4.4. This illustrates the sum of the first thousand terms of a fractal sine series for $T_{FG_2}(x)$ on [0, 1]. Compare with Fig. 3. Note the "fractal Gibbs effect 8" that has resulted in the vertical line.

tent function using fractal orthogonal functions $\widetilde{e}_n$. The approximations use 3 (red), 5 (green), 7 (blue), 20 (black) terms. The Fourier series are (up to a normalization constant)

$$\sum_{n=1}^{k} \frac{2\sin(\pi n/2) - \sin(\pi n)}{n^2}\, e_n(x)$$

$$\text{and} \quad \sum_{n=1}^{k} \frac{2\sin(\pi n/2) - \sin(\pi n)}{n^2}\, \widetilde{e}_n(x).$$

Example 4.4 (Function with a dense set of discontinuities)**.** Consider the following approximation of a function with a dense set of discontinuities. Let $\psi \in L^2[0,1]$ be defined by $\psi(x) = x$ for all $x \in [0,1]$. Then $\phi_i = U_{FG_i}\psi$, $i = 1, 2$, is given by $\phi_i(x) = (U_{FG_i}\psi)(x) = \psi(T_{G_iF}(x)) = T_{G_iF}(x)$, which has a dense set of discontinuities (see Example 3.3). It follows, by a short calculation using statement 2 of Theorem 2.4, that the coefficients in the $\widehat{e}_n$ and $\widetilde{e}_n$ Fourier series expansion of ϕ_i are the same as the coefficients in the e_n expansion for ψ. Therefore the fractal Fourier series expansions for ϕ_i, $i = 1, 2$, are

$$\frac{2}{\pi}\sum_{n=1}^{\infty} \frac{-\cos(\pi n)}{n}\, \widehat{e}_n(x), \qquad \text{and} \qquad \frac{2}{\pi}\sum_{n=1}^{k} \frac{-\cos(\pi n)}{n}\, \widetilde{e}_n(x),$$

respectively. Sums with 10, 30, and 100 terms are shown in red, green, and blue, respectively, in Fig. 14 for ϕ_1, and in Fig. 15 for ϕ_2, using the first 1000 terms of the series.

4.2. Legendre polynomials.

The Legendre polynomials are the result of applying Gram-Schmidt orthogonalization to $\{1, x, x^2, \dots\}$, with respect to Lebesgue measure on $[-1, 1]$. Denote the Legendre polynomials shifted to the interval [0, 1] by $\{P_n(x)\}_{n=0}^{\infty}$. They form a complete orthogonal basis for $L^2[0,1]$, where the inner product is

$$\langle \psi, \varphi \rangle = \int_0^1 \overline{\psi(x)}\varphi(x)dx.$$

In this case each of the unitary transformations U_{FG_i}, $i = 1, 2$ associated with Example 3.3 maps $L^2[0,1]$ to itself, and we obtain the fractal Legendre polynomials

$$P_n^{FG_i}(x) = P_n(T_{GF}(x)).$$

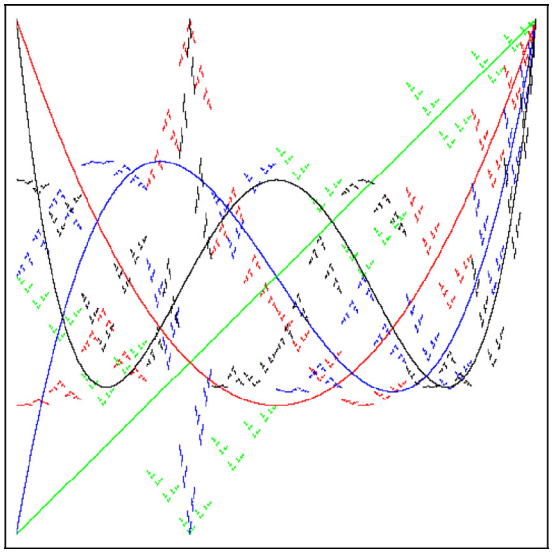

Fig. 16. Legendre polynomials and their fractal counterparts corresponding to T_{FG_1}. Both sets of functions form orthogonal basis sets with respect to Lebesgue measure on the interval $[-1, 1]$. See also Fig. 17.

Figs. 16 and 17 illustrate the Legendre polynomials and their fractal counterparts. Fig. 16 shows the fractal Legendre polynomials $P_n^{FG_1}(x)$ and Fig. 17 shows the fractal Legendre polynomials $P_n^{FG_2}(x)$.

4.3. The action of the unitary operator on Haar wavelets.

With F, G_2 and $T = T_{FG_2} : [0,1] \to [0,1]$ as previously defined, let $U = U_{FG_2} : L^2[0,1] \to L^2[0,1]$ be the associated (self-adjoint) unitary transformation. Let $I_\emptyset = [0,1]$ and $H_\emptyset : \mathbb{R} \to \mathbb{R}$ be the Haar mother wavelet defined by

$$H_\emptyset(x) = \begin{cases} +1 \text{ if } x \in [0, 0.5), \\ -1 \text{ if } x \in [0.5, 1), \\ 0 \text{ otherwise.} \end{cases}$$

For $\sigma \in \{0,1\}^k$, $k \in \mathbb{N}$, write $\sigma = \sigma_1\sigma_2\dots\sigma_k$ and $|\sigma| = k$. If $|\sigma| = 0$ then $\sigma = \emptyset$, the empty string. Also let $I_\sigma = h_{\sigma_1} \circ h_{\sigma_2} \circ \cdots \circ h_{\sigma_k}(I_\emptyset)$, where $h_0 = f_1$ and $h_1 = f_2$, and let $A_\sigma : \mathbb{R} \to \mathbb{R}$ be the unique affine

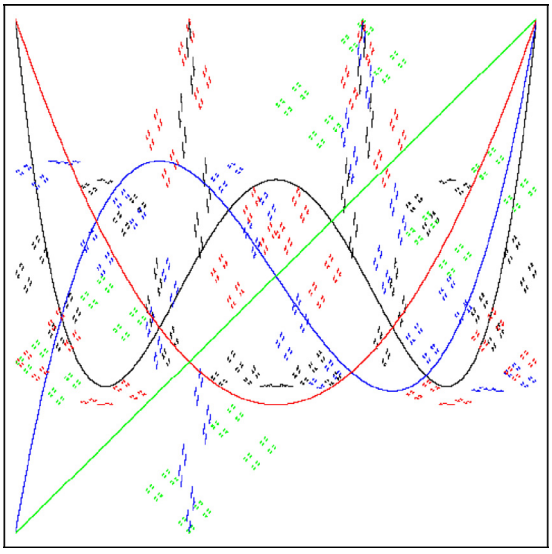

Fig. 17. Legendre polynomials and their fractal counterparts corresponding to T_{FG_2}. See also Fig. 16.

map such that $A_\sigma(I_\emptyset) = I_\sigma$. With this notation, the **standard Haar basis**, a complete orthonormal basis for $L^2[0, 1]$, is

$$\{H_\sigma : \sigma \in \{0,1\}^k, k \in \mathbb{N}\} \cup \{H_\emptyset(x)\} \cup \{\mathbf{1}\},$$

where $\mathbf{1}$ is the characteristic function of $[0, 1)$ and $H_\sigma : [0, 1) \to \mathbb{R}$ is defined by

$$H_\sigma(x) = 2^{|\sigma|/2} H_\emptyset(A_\sigma^{-1}(x)).$$

There is an interesting action of $U = U_{FG_2}$ on Haar wavelets. The operator U permutes pairs of Haar wavelets at each level and flips signs of those at odd levels, as follows. By calculation, for $\sigma \in \cup_{k\in\mathbb{N}}\{0,1\}^k$,

$$UH_\sigma = (-1)^{|\sigma|} H_{\sigma'}$$

where $|\sigma| = |\sigma'|$ and $\sigma'_l = (-1)^{l+1}\sigma_l + (1 + (-1)^k)/2$ for all $l = 1, 2, \ldots, |\sigma'|$, $UH_\emptyset = H_\emptyset$, and $U1 = 1$. It follows that if $f \in L^2[0, 1]$ is of the special form

$$f = a_\emptyset H_\emptyset + \sum_{\sigma\in\cup_{k\in\mathbb{N}}\{0,1\}^{2k}} c_\sigma (H_\sigma + H_{\sigma'}),$$

then $Uf = f$ and $f \circ T = f$. Such signals are invariant under U. It also follows that if P is the projection operator that maps $L^2[0, 1]$ onto the span of all Haar wavelets down to a fixed depth, then $U^{-1}PU = P$.

4.4. Unitary transformations from the Hilbert mapping and its inverse

This continues Example 3.5, where the fractal transformations $h := T_{FG}$ and $h^{-1} := T_{GF}$ are the Hilbert mapping and its inverse, both of which preserve Lebesgue measure and are mappings between one and two dimensions. The unitary transformations $U_{FG} : L^2([0, 1]) \to L^2([0, 1]^2)$ and $U_{GF} : L^2([0, 1]^2) \to L^2([0, 1])$ are given by

$$U_{FG}(f) = f \circ h^{-1}, \qquad U_{GF}(f) = f \circ h.$$

A *picture* can be considered as a function $f : [0, 1]^2 \to \mathbb{R}$, where the image of a point x in $\mathbb{R}^2$ gives a gray scale value. Three such functions (or one function $f : [0, 1]^2 \to \mathbb{R}^3$) can be combined to give RGB colors. The top image of Fig. 18 is such a picture given by a function $f : [0, 1]^2 \to \mathbb{R}^3$. The bottom image is the function (picture) $U_{GF} f = f \circ h$ transformed by the unitary operator.

Fig. 18. See Section 4.4.

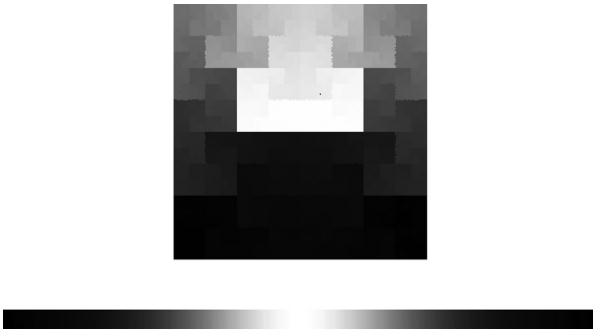

Fig. 19. The bottom band shows the graph of $\sin(\pi x)$ with function values represented by shades of grey. The top band shows the graph of $h(sin(\pi x))$, where h is the Hilbert function.

Fig. 20. The top image illustrates the graph of $f(x, y) = \sin(\pi x)$ for $x, y \in [0, 1]^2$. The band at the bottom illustrates the graph of the pull-back $f \circ h : [0, 1] \to [-1, 1]$, which is continuous, in contrast to the situations in Fig. 18.

Since the Hilbert map $h : [0, 1] \to [0, 1]^2$ is continuous, if $f : [0, 1]^2 \to \mathbb{R}$ is also continuous, then so is the pull-back $U_{GF}(f) = f \circ h : [0, 1] \to \mathbb{R}^1$. Therefore, any orthonormal basis $\{\psi_n : [0, 1]^2 \to \mathbb{R}\}$ on $[0, 1]$ consisting of continuous functions is mapped, via the unitary operator U_{GF}, to an orthonormal basis $\{\psi_n \circ h : [0, 1] \to \mathbb{R}\}$ consisting of continuous functions. In the other direction, the image under U_{FG} of an orthonormal basis consisting of continuous functions on $[0, 1]$ may not comprise continuous functions on $[0, 1]^2$. Figs. 19 and 20 illustrate this.

In Fig. 21, the right image represents the function $f : [0, 1]^2 \to [-1, 1]$ defined by $f(x, y) = \sin(\pi x)\sin(\pi y)$. The left image represents the function $g : [0, 1] \to [-1, 1]$ defined by the continuous function $g(x, y) = U_{GF}(f) = f \circ h(x)$ where $h : [0, 1] \to [0, 1]^2$ is the Hilbert function. The set of functions in the orthogonal basis $\{\sin(n\pi x)\sin(m\pi y) : n, m \in \mathbb{N}\}$ for $L^2([0, 1]^2)$ (w.r.t. Lebesgue two-dimensional measure) is fractally transformed via the Hilbert mapping to an othogonal basis for $L^2[0, 1]$ (w.r.t. Lebesgue one-dimensional measure). In contrast to the situation in Section 4.1, these fractal sine functions are continuous.

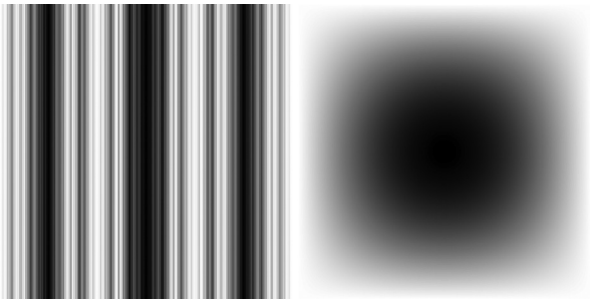

Fig. 21. The right image represents the graph of $f:[0,1]^2 \to [-1,1]$ defined by $f(x,y) = \sin(\pi x)\sin(\pi y)$. The left image represents the graph of $g:[0,1]^2 \to [-1,1]$ defined by the continuous function $g(x,y) = U_{GF}(f) = f \circ h(x)$ where $h:[0,1] \to [0,1]^2$ is the Hilbert function.

Acknowlegements

We thank an anonymous referee for some helpful corrections. We acknowledge support for this work by Australian Research Council grant DP130101738. This work was also partially supported by a grant from the Simons Foundation (322515 to Andrew Vince). We thank Louisa Barnsley for her help with this paper.

References

[1] Atkins R, Barnsley MF, Vince A, Wilson D. A characterization of hyperbolic affine iterated function systems. Topology proceedings 2010;36:189–211.
[2] Bandt C, Graf S. Self-similar sets 7. a characterization of self-similar fractals with positive hausdorff measure. Proc Am Math Soc 1992;114:995–1001.
[3] Bandt C, Hung NV, Rao H. On the open set condition for self-similar fractals. Proc Am Math Soc 2005;134:1369–74.
[4] Barnsley MF. Fractals everywhere. 2nd ed. Cambridge, MA: Academic Press; 1993.
[5] Barnsley MF. Theory and applications of fractal tops. In: Fractals in engineering: new trends in theory and applications. Springer-Verlag; 2005. p. 3–20.
[6] Barnsley MF. Superfractals. Cambridge University Press; 2006.
[7] Barnsley MF. Transformations between self-referential sets. Math Monthly 2009:291–304.
[8] Barnsley MF, Harding B, Igudesman K. How to transform and filter images using iterated function systems. SIAM J Imaging Sci 2011;4(4):1001–28.
[9] Barnsley MF, Vince A. Fractal homeomorphism for bi-affine iterated function sytems. Int J Appl Nonlinear Sci 2012;1:3–19.
[10] Barnsley MF, Vince A. Developments in fractal geometry. Bull Math Sci 2013;3:299–348.
[11] Barnsley MF, Vince A. Symbolic iterated function systems, fast basins and fractal manifolds. SIGMA 2015;11:21. 084
[12] Elton JH. An ergodic theorem for iterated maps. Ergodic Theor Dynam Syst 1987;7:481–8.
[13] Falconer K. Fractal geometry: mathematical foundations and applications. John Wiley & Sons; 1990.
[14] Graf S. On bandt's tangential distribution for self-similar measures. Monatsh Math 1995;120:223–46.
[15] Hilbert D. Über die stetige abbildung einer linie auf ein flächenstück. Mathematiche Annalen 1891;38:459–60.
[16] Hutchinson J. Fractals and self-similarity. Indiana Univ Math J 1981;30:713–47.
[17] Kigami J. Analysis on fractals. Cambridge University Press; 2001.
[18] Kigami J. Volume doubling measures and heat kernel estimates on self-similar sets. Memoirs Am Math Soc 2009;199.932:1–94.
[19] Morán M. Dynamical boundary of a self-similar set. Fundamenta Mathematicae 1999;160:1–14.
[20] Morán M, Rey J. Singularity of self-similar measures with respect to hausdorff measures. Trans Amer Math Soc 1998;350:2297–310.
[21] Moran PAP. Additive functions of intervals and hausdorff measure. Math Proc Cambridge Phil Soc 1946;42:15–23.
[22] Patzschke N. Self-conformal multifractal measures. Adv Appl Math 1997;19:486–513.
[23] Schief A. Separation properties for self-similar sets. Proc Am Math Soc 1994;122:111–15.
[24] Schief A. Self-similar sets in complete metric spaces. Proc Am Math Soc 1996;124:481–90.
[25] Sagan H. Space-filling curves. Universitext. New York: Springer-Verlag; 1994.
[26] Staiger L. How large is the set of disjunctive sequences. In: Combinatorics, computability and logic. In: Discrete mathematics and theoretical computer science; 2001. p. 215–25.
[27] Strichartz RS. Differential equations on fractals. New Jersey: Princeton University Press; 2006.